

# Wavelet based Method of Mapping the Brain Activity Waves Travelling over the Cerebral Cortex

Bozhokin Sergey<sup>a</sup>, Suslova Irina<sup>b</sup> and Tarakanov Daniil

Peter the Great Polytechnic University, Polytechnicheskaya str. 29, Saint-Petersburg, Russia

**Keywords:** Continuous Wavelet Transform, Spectral Integrals, Cortical Travelling Waves.

**Abstract:** The brain electroencephalogram is treated as a set of electrical activity bursts in various spectral ranges. Spectral integrals calculated by the wavelet transform method are used to study time–frequency properties of such bursts. The mathematical theory has been developed to describe quantitatively the change in the shape of EEG bursts while their propagating along the cerebral cortex. The proposed model of neural activity uses nonlinear approximation of EEG record as a sum of several Gaussian peaks moving along different trajectories with different speeds. Such model together with the continuous wavelet transform provides an opportunity to receive analytical solutions. The proposed method allows us to draw the maps showing the trajectories of EEG bursts moving along the cerebral cortex. It also becomes possible to study the change in the shape of bursts in the process of their motion. The method was applied to study EEG records of a healthy subject at rest with his eyes closed.


## 1 INTRODUCTION


At the macro level, the electrical activity of numerous neural ensembles is recorded as an electroencephalogram signal (EEG) from many brain channels in different spectral ranges  $\mu = \{\delta, \theta, \alpha, \beta\}$ , where  $\delta$ -rhythm (0,5–4 Hz),  $\theta$ -rhythm (4–7,5 Hz),  $\alpha$ -rhythm (7,5–14 Hz),  $\beta$ -rhythm (14–30 Hz) (Nunez and Srinivasan 2006; Gnezditskii 2004; Ivanitsky et al. 2009; Tong and Thakor 2009; Zenkov 2013). This is the most common non-invasive research method. It is known that EEG is an inherently unsteady process. Even at rest, in the absence of any external stimuli, we observe numerous temporary bursts due to spontaneous fluctuations in the level of electrical activity caused by synchronization and desynchronization processes associated with individual characteristics of mental activity during registration (Hramov et al. 2015).

EEG structure represents various forms of oscillatory patterns related to the electrical activity of neural ensembles and reflecting the functional states of the brain (Borisyyuk and Kazanovich 2006; Quiles et al. 2011; Chizhov and Craham 2008; Tafreshi et al.

2019). It was shown (Kaplan and Borisov 2003) that the amplitude, temporal, and spatial characteristics of neural activity segments indicate the rate of formation, the lifetime, and the rate of decay of neural ensembles. In this work, it is noted that the duration of the quasi-stationary segments of alpha activity is approximately equal to  $\tau \approx 300 - 350$  ms depending on the channel. This value exceeds approximately three times the characteristic period of alpha oscillations  $T_\alpha = 1/f_\alpha \approx 100$  ms, where  $f_\alpha = 10$  Hz. As a rule, to analyse the variation in spectral properties of the signal, the Short Time Fourier Transform (STFT) is applied. We have good resolution of temporal behaviour of the signal in the case when the window duration  $W$  satisfies the condition  $1/f_\alpha \ll W \ll \tau$ . However, in the case when the condition  $\tau \approx 3T_\alpha$  is satisfied, the application of the STFT method leads to incorrect determination of spectral properties.

One of the most difficult tasks in EEG processing is to determine the localization of spatial and temporal sources of neural activity from the signals recorded on the outer surface of the skull. Such a problem relates to the inverse problems of mathematical physics. Even in the case of the most simplified model of neural activity sources as electric dipoles located in a homogeneous

<sup>a</sup>  <https://orcid.org/0000-0001-5653-6574>

<sup>b</sup>  <https://orcid.org/0000-0002-4497-1867>

sphere, the problem does not have a unique solution. The real topology of the cortex has a complex structure with a lot of convolutions and furrows. In addition, we should notice that the spatial form of brain anatomical structures is individual for each person. In solving these problems, it is also necessary to take into account the anisotropy of brain conductivity in various directions (Lopes de Silva 1991; Pfurtscheller et al. 1990; Verkhlyutov et al. 2019; Ozaki et al. 2012).

The experiments show the successive shifts of electrical activity maxima over different trajectories. This movement can be interpreted as wave propagation in certain direction along the surface of the brain. The work (Manjarrez et al., 2007) calculated the trajectories of waves in  $\alpha$ -rhythm range, originating mainly in the frontal or occipital region. The trajectories of these waves always cross the central zones of the brain. The characteristic velocity of such waves is  $2.1 \pm 0.29$  ms. Currently, it is believed that EEG wave generators are a group of combined nerve cells (columns or dipoles) that transmit their excitation to neighboring neural centers (Ng et al. 2014).

The Fast Fourier transform (STFT) with dividing the entire EEG record into separate epochs lasting 4 s is used to solve the problem of the propagation of disturbances over the surface of the brain in the articles (Massimini et al. 2004; Riedner et al. 2007). By using cross-correlation analysis (Kulaichev 2016), the work (Belov et al. 2014) studies the influence of interhemispheric asymmetry and the patient's psychological type on the characteristics of the "traveling EEG wave". The method of segmentation of EEG signals with the subsequent use of indicators of coherence and synchronism (Phase-locking value) was used to quantify the performance of traveling EEG waves in (Trofimov et al. 2015; Bahramisharif et al. 2013). In the article (Getmanenko et al. 2006), temporary mismatches in the electrical activity of the cerebral cortex are calculated from the shift in the maximum of cross-correlation function. However, it was shown (Kulaichev 2016) that the coherence value of the two signals depends very much on the averaging procedure, on the choice of the window size, on the window function, on the magnitude of the window pitch shift. Consequently, the coherence value cannot be considered as a sufficiently accurate quantitative measure of the correlation of two signals  $Z_I(t)$  and  $Z_K(t)$ , where  $I$  and  $K$  are the numbers of EEG channels.

The velocities of travelling waves (TW) propagation in various spectral ranges are calculated in (Patten et al. 2012). In this work, it was shown that  $\alpha$ -waves (the speed of 6.5 m/s) propagate faster than  $\theta$ -waves having the speed of 4 m/s. According to the

theory of diffuse signal transmission through nerve tissue (Lopes da Silva 1991; Pfurtscheller and Lopes da Silva 1999), the signal pathway consists of many fibers with different conduction speeds. TW are associated with switching the activity of different brain centers. With each such switching, the outburst of neural activity being compact at the beginning stretches in time and decreases in amplitude due to the dispersion of the medium.

Currently, the dynamics of the cerebral cortex of clinical patients is often analyzed by using intracranial electrocorticogram record (ECoG) (Zhang et al. 2018; Belov et al. 2016). The review (Muller et al. 2018) presents the conceptual basis of the traveling wave phenomenon as a response generated by intra-cortical contours to external stimuli. The analysis of traveling waves as a non-stationary process caused by the internal or external stimulus allows us to obtain information not only about the spatial localization of the stimulus, but also about the time it occurred (Muller et al. 2018; Patten et al. 2012). When studying the memory mechanisms (Zhang et al. 2018), the traveling waves were identified at different frequencies in a wide frequency range (from 2 to 15 Hz) and with various electrode configurations, in most cases, traveling waves propagate from the posterior to the anterior regions of the brain (Voytek et al. 2010; Zhang et al. 2018). The main mathematical tools for studying traveling waves are neural network methods (Villacorta et al. 2013; Terman et al. 2001). The wavelet transform method (Patten et al. 2012; Alexander et al. 2013; Zhang et al. 2018) is also widely used in the quantitative description of the dynamics of neural ensembles.

This work proposes a new mathematical model of neural activity based on the nonlinear approximation of each EEG burst in the form of the sum of moving Gaussian peaks. The maxima of electrical activity bursts calculated in all spectral ranges  $\mu = \{\delta, \theta, \alpha, \beta\}$  take place at different points in time. The movements of the activity maxima calculated for a given channel show the trajectories of EEG waves propagating through the cerebral cortex. Using the proposed special model and wavelet based mathematical tools, the trajectories and speeds of neural activity bursts along the cerebral cortex can be found. The studies have been carried out by calculating the correlation in time of the electrical activity bursts in various EEG channels (Bozhokin and Suslova 2015) based on the continuous wavelet transform method (CWT –continuous wavelet transform) and on the analysis the time variation of spectral integrals.

The advantage of using the wavelet methods in this article is the ability to correctly describe the behavior in time of the EEG activity bursts in any spectral range  $\mu = \{\delta, \theta, \alpha, \beta\}$ . This approach gives the opportunity to study EEG bursts in all spectral ranges and their evolution in time. The new model of EEG bursts together with the new techniques related to CWT allows us finding both the trajectories of the motion and the change in the shape of EEG bursts while their travelling along the cerebral cortex. In addition, the proposed model gives analytical solution, which can be used to check the numerical procedures. Thus, we can consider the proposed methods as giving some additional information and capabilities in the study of brain waves propagation.

## 2 MATERIALS AND METHODS

In this work, we processed the spontaneous EEG of a healthy subject at rest with his eyes closed (Anodina-Andrievskaya et al. 2011). Background EEG activity is a desynchronized activity of neural ensembles of the cerebral cortex. In addition to the background activity, the EEG signal contains various oscillatory patterns, which are continuously appearing and disappearing bursts of rhythms characterizing the coherent electrical activity of neural ensembles. When recording the EEG, the standard channels were used according to the 10-20% scheme, where the index  $J=1,2, \dots, 21$  takes the values  $J = \{\text{Fp1, Fpz, Fp2; F7, F3, Fz, F4, F8; T3, C3, Cz, C4, T4; T5, P3, Pz, P4, T6; O1, Oz, O2}\}$ . The shifts of the maxima of electrical activity on the cerebral cortex are approximately equal to 5-10 ms, therefore, the signal sampling frequency should be at least = 500 Hz. The duration of the EEG recording is approximately equal to  $T = 30$  s.

### 2.1 Continuous Wavelet Transform (CWT) and Spectral Integrals

The modified form  $V^{(J)}(\nu, t)$  of the continuous wavelet transform (CWT) for an EEG signal  $Z^{(J)}(t)$  from EEG channel  $J$ , depending on the frequency  $\nu$  and time  $t$ , as well as the explicit form of the Morlet mother wavelet function, which we will use in this paper, are given in (Bozhokin and Suvorov 2008; Bozhokin et al. 2017). Fig.1 shows the absolute value  $|V^{(J)}(\nu, t)|$  for the occipital channel  $J = O_z$ . The spectral integrals  $E_\mu(J, t)$ , which represent the local density of signal energy spectrum integrated over the given frequency range  $\mu$ , are determined in (Bozhokin and Suslova 2015).

We define a burst of EEG activity in  $\mu$ -frequency range as the appearance and disappearance of a group of waves different from the background EEG in frequency, shape and amplitude. This can continue for a certain period of time. The maximum of the electrical activity of such a burst is localized at a certain point in time  $t_{max}$  (the center of the burst).

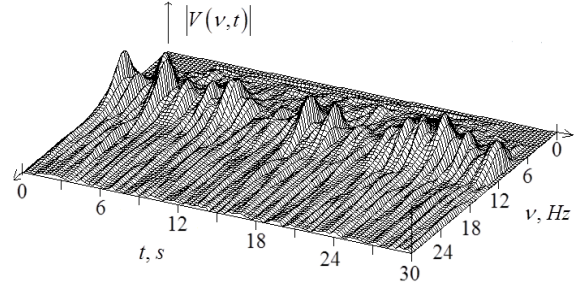


Figure 1: CWT modulus  $|V^{(J)}(\nu, t)|$  depending on frequency  $\nu$  and time  $t$  for the EEG channel  $J = O_z$ .

The burst has its beginning and end, and we can calculate the time-behavior of the local frequency  $F_\mu(t)$ , which corresponds to the maximal value of  $|V^{(J)}(\nu, t)|$  at fixed moment of time in the given frequency range  $\mu$ . Fig.1 shows that the real EEG signal from the given brain channel can be treated as a set of EEG activity bursts taking place at different time moments in different spectral ranges.

Fig.2 shows spectral integrals  $E_\alpha(J, t)$  in  $\alpha$ -range for three brain channels  $J = \{F_{pz}; C_z; O_z\}$ . Based entirely on Fig.2, we conclude that in  $\alpha$ -range, brain activity is a sequence of bursts (in this case, sleep spindles), and the intensity of  $\alpha$ -bursts in the occipital channel is much higher than in the frontal. Fig.2 demonstrates the strong non-stationarity of the EEG, expressed in the fact that the amplitude and spectral properties of such a signal strongly depend on time.

By examining the performance of spectral integrals  $E_\alpha(J, t)$ , and by setting the cut off level relative to the maximum level, we can represent the EEG in the entire observation interval for each channel  $J$  as a set of bursts with certain duration.

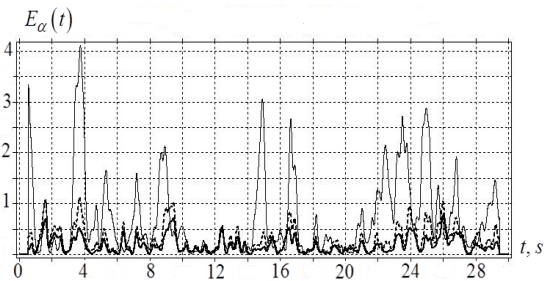


Figure 2: Spectral integrals  $E_\alpha(J, t)$  depending on  $t, s$  for  $O_z$ -brain channel (thin line),  $C_z$  (dot line), and  $F_{pz}$  (bold line).

The maximum of each burst is also localized in time and frequency. The wavelet images of the EEG signals from the other brain channels are similar in general, but different in patterns. The bursts differ in the form, and their maximums also vary in values and times of occurrence (Fig.1). The quantitative parameters characterizing each burst, and their classification are given in (Bozhokin and Suslova 2014; Bozhokin and Suslova 2015).

## 2.2 Mathematical Model of a Complex EEG Burst

Let us develop a mathematical theory, which will allow us to describe quantitatively the change in the shape of EEG bursts while their moving over the cerebral cortex. In the spectral range  $\mu = \{\alpha, \beta, \gamma, \delta\}$ , the EEG burst detected in the given brain channel  $J$  is characterized by spectral integral  $E_\mu(J, t)$ . First, to develop a mathematical model  $\tilde{E}_\mu(J, t)$  of the burst, we consider a single Gaussian peak

$$G(\vec{g}, t) = a_1 \exp[-(t - b_1)^2 / 2c_1^2] \quad (1)$$

depending on time  $t$ , and the vector  $\vec{g}_1 = (a_1; b_1; c_1)$  with the parameters:  $a_1$  – the amplitude,  $b_1$  – the time localization center,  $c_1$  – the peak's width. Then, we represent mathematical model  $\tilde{E}_\mu(J, t)$  as a sum of  $n$  Gaussian peaks  $G(\vec{g}_s, t)$ :

$$\tilde{E}_\mu(J, t) = \sum_{s=1}^n G_\mu(J, \vec{g}_s, t), \quad (2)$$

where  $\vec{g}_s$  is the vector corresponding to  $s$ -peak. As the simplest example, we take the sum of three Gaussian peaks (with nine parameters  $\vec{g}_1; \vec{g}_2; \vec{g}_3$ ) to simulate  $\alpha$ -burst ( $\mu = \alpha$ ). The parameters of the Gaussian peaks for a fixed burst are selected from the condition

$$\Delta^2 = \frac{1}{N} \sum_{i=1}^N [E_\alpha(J, t_i) - \tilde{E}_\alpha(J, t_i)]^2 \rightarrow \min \quad (3)$$

where  $E_\alpha(J, t)$  is the burst observed experimentally;  $\tilde{E}_\alpha(J, t)$  is the theoretical model (2);  $\Delta$  is the standard error of approximation. In (3) the value of  $\Delta$  represents the standard error of the approximation. The summation in (3) is carried out over all time instants  $t_i$  for the selected burst localized in the time interval  $[t_1; t_2]$  in the alpha range. To find the minimum (3), we applied the modified Newton method with accuracy control. The program was tested on the example of determining the parameters of Gaussian peaks, when the program

input  $E_0(t)$  consists of three ideal Gaussian peaks with the parameters  $\vec{g}_i = (a_i; b_i; c_i)$  (1) close to the real situation:  $\vec{g}_1 = (0.49938; 8.2785; 0.15001)$ ;  $\vec{g}_2 = (1.5194; 8.6258; 0.11486)$ ;  $\vec{g}_3 = (2.0357; 8.9427; 0.16810)$ . The result of the program is shown in Fig.3. Analysing this dependence, it is important to note: the true peaks of the Gaussian curves and the peaks of the signal  $E_0(t)$  can occupy different positions in time. This conclusion will be important in the study of real records of EEG activity bursts. In addition, a slight change in the values of  $\vec{g}_i = (a_i; b_i; c_i)$  can significantly change the topology of the overall picture  $E_0(t)$ . The approximation of the system of nonlinear equations  $\tilde{E}_0(t)$  using the nonlinear approximation program (3) reproduces, with accuracy to the fifth decimal place, the parameters  $\vec{g}_1; \vec{g}_2; \vec{g}_3$  of the test signal  $E_0(t)$ . The mean square error between  $\tilde{E}_0(t)$  and  $E_0(t)$  is  $\Delta = 8.3 \cdot 10^{-6}$ , therefore, the curves in Fig.3 merge.

To increase the accuracy of approximation (3), the experimentally observed values  $E_\alpha(J, t)$  were interpolated using the theory of splines. This led to the fact that the signal sampling step  $\Delta t = 2$  ms was reduced by 20 times. The calculations showed that most real EEG bursts are satisfactorily described by three-Gaussian approximation ( $n = 3$ ), and the standard deviation between the experimental and theoretical models is  $\Delta < 0.03$ .

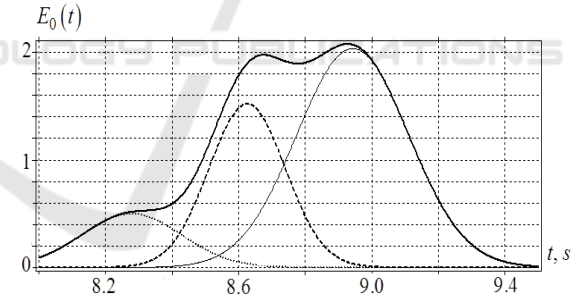


Figure 3: Three Gaussian peaks with the parameters  $\vec{g}_1; \vec{g}_2; \vec{g}_3$  are shown by dots, dashes, and thin lines, respectively. The bold line corresponds to the sum of three ideal Gaussian peaks with the parameters  $\vec{g}_1; \vec{g}_2; \vec{g}_3$ . The curve  $E_0(t)$  and its approximation  $\tilde{E}_0(t)$  merge entirely into the bold line.

## 2.3 Results

### 2.3.1 Comparison of EEG Simulation Results and Experimental Data

Let us construct the mathematical model of EEG burst with the duration  $[8-9.15$  s] in  $\alpha$ -spectral range, and follow the change in the shape of this burst while

moving between two occipital electrodes  $J = O_Z \rightarrow J = O_2$ .

For the burst in the interval [8-9.15 s], the difference (3) between the model  $\tilde{E}_\alpha(J, t)$  and experimental  $E_\alpha(J, t)$  is  $\Delta(O_2) \approx 0.024$ , and  $\Delta(O_Z) \approx 0.027$ .

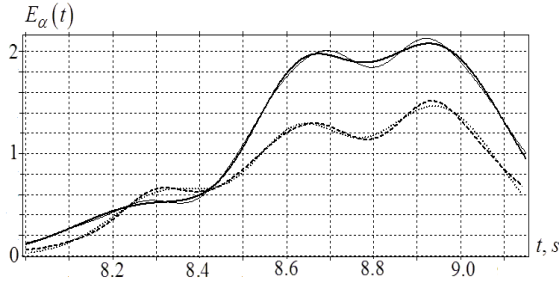


Figure 4: Comparison of the spectral integrals  $E_\alpha(J, t)$  obtained for the experimental record of EEG burst in the interval [8–9.15 s] with their mathematical models  $\tilde{E}_\alpha(J, t)$ : thin line  $-E_\alpha(O_Z; t)$ ; bold line  $-\tilde{E}_\alpha(O_Z; t)$ ; dash line  $-E_\alpha(O_2; t)$ ; dot line  $-\tilde{E}_\alpha(O_2; t)$ .

When the burst propagates in the direction  $O_Z \rightarrow O_2$ , the behavior of three Gaussian peaks, which form the model burst in the range [8–9.15 s], is different (Fig.4). The amplitude of the left peak increases:  $a_1(O_2)/a_1(O_Z) = 1.26$ , the time shift between the peaks  $O_Z \rightarrow O_2$  is positive  $\Delta t = b_1(O_2) - b_1(O_Z) = 0.0424$  s. The amplitude of the central peak decreases  $a_2(O_2)/a_2(O_Z) = 0.74$ . The time shift of the central peak is negligible  $\Delta t = b_2(O_2) - b_2(O_Z) = -0.004$ . The amplitude of the right peak decreases  $a_3(O_2)/a_3(O_Z) = 0.712$ , and its maximum lags behind the maximum of the central peak  $\Delta t = b_3(O_2) - b_3(O_Z) = 0.0037$ . The characteristic widths of all three peaks ( $c_1; c_2; c_3$ ) during their propagation  $O_Z \rightarrow O_2$  vary slightly.

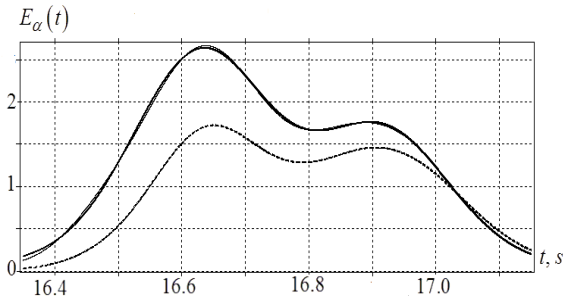


Figure 5: Comparison of the spectral integrals  $E_\alpha(J, t)$  obtained for the experimental record of EEG burst in the interval [16.2-17.2 s] with their mathematical models  $\tilde{E}_\alpha(J, t)$ : thin line  $-E_\alpha(O_Z; t)$ ; bold line  $-\tilde{E}_\alpha(O_Z; t)$ ; dash line  $-E_\alpha(O_2; t)$ ; dot line  $-\tilde{E}_\alpha(O_2; t)$ .

Fig.5 represents the curves  $E_\alpha(J, t)$  and  $\tilde{E}_\alpha(J, t)$  for  $O_Z$  and  $O_2$  channels, which correspond to the burst in the time interval [16.3-17.2 s] (compare with Fig.4). For such a burst, the agreement between experiment and theory is better:  $\Delta(O_2) \approx 0.003$ ,  $\Delta(O_Z) \approx 0.02$ , as compared to that in the interval [8–9.15 s].

For the burst in the interval [16.2-17.2 s] propagating in the direction  $O_Z \rightarrow O_2$  (Fig.5), the amplitude of the left main peak decreases:  $\frac{a_1(O_2)}{a_1(O_Z)} = 0.258$ . The time shift between two main peaks is positive:  $\Delta t = b_1(O_2) - b_1(O_Z) = 0.007$  s. Provided the distance between the nearest ( $O_Z \rightarrow O_2$ ) electrodes  $L = 5$  cm, the propagation velocity of this alfa-rhythm peak is  $V_\alpha(O_Z \rightarrow O_2) = L/\Delta t$ , where  $V_\alpha = 7.4$  ms. Note that the amplitude of the rightmost peak of this burst increases slightly:  $a_2(O_2)/a_2(O_Z) = 1.06$ . The time shift between the third peaks during the transition  $O_Z \rightarrow O_2$  is also positive:  $\Delta t = b_3(O_2) - b_3(O_Z) = 0.002$  s, and its width becomes larger  $c_3(O_2)/c_3(O_Z) = 1.21$ . Such an expansion of the right peak of the burst and a slight increase in its amplitude can be observed in Fig.5 at time  $t \approx 17.1$  s.

### 2.3.2 The Trajectories of the EEG Bursts in $\alpha$ -range and the Map of Cerebral Cortex Electrical Activity

Let us consider the methodology for calculating the propagation rates of bursts moving along the cerebral cortex on the example of EEG bursts in  $\alpha$ -range.) We study two bursts in  $\alpha$ -range but in different time intervals: one evolves in the time interval [8–9.15 s] (Fig.4), the second in [16.3–17.2 s] (Fig.5). For each brain channel, the coordinates of the maximum value of the spectral integral in the given time interval are indicated in brackets.

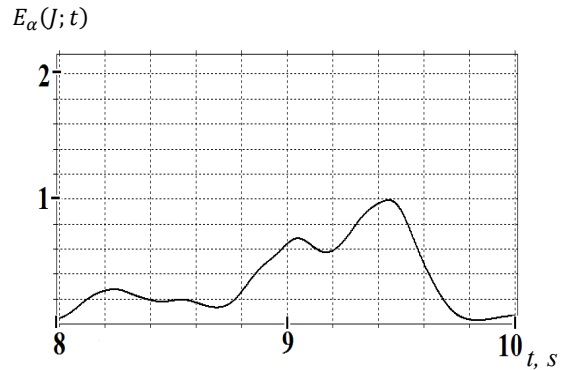


Figure 6a: Spectral integral in the channel  $C_3$  (9.444;0.998) in the interval [8–9.15 s].

$E_{\alpha}(J; t)$

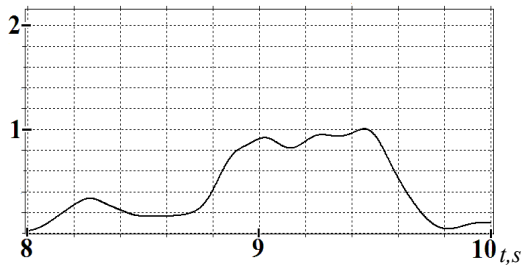


Figure 6b: Spectral integral in the channel  $C_z$  (9.456;1.003) in the interval [8–9.15 s].

$E_{\alpha}(J; t)$

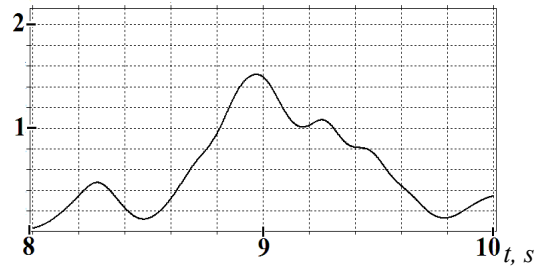


Figure 6f: Spectral integral in the channel  $P_4$  (8.970;1.518) in the interval [8–9.15 s].

$E_{\alpha}(J; t)$

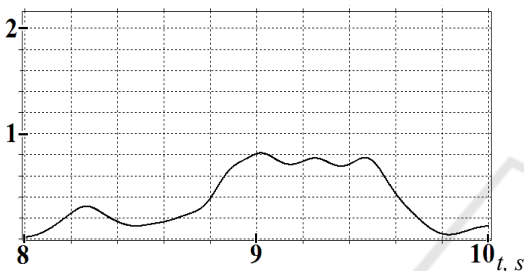


Figure 6c: Spectral integral in the channel  $C_4$  (9.018;0.815) in the interval [8–9.15 s].

$E_{\alpha}(J; t)$

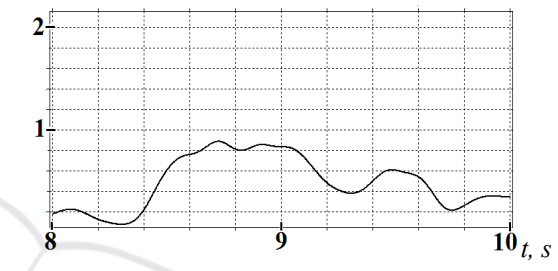


Figure 6g: Spectral integral in the channel  $0_1$  (8.724;0.888) in the interval [8–9.15 s].

$E_{\alpha}(J; t)$

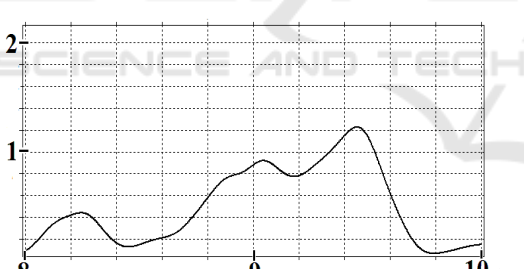


Figure 6d: Spectral integral in the channel  $P_3$  (9.454;1.226) in the interval [8–9.15 s].

$E_{\alpha}(J; t)$

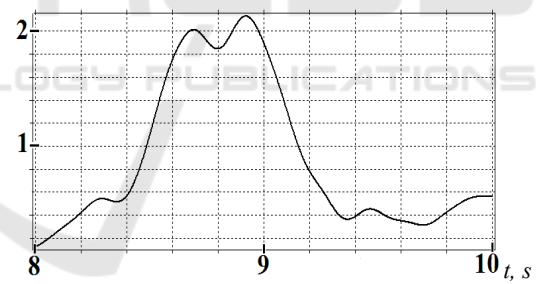


Figure 6h: Spectral integral in the channel  $0_z$  (8.920;2.13) in the interval [8–9.15 s].

$E_{\alpha}(J; t)$

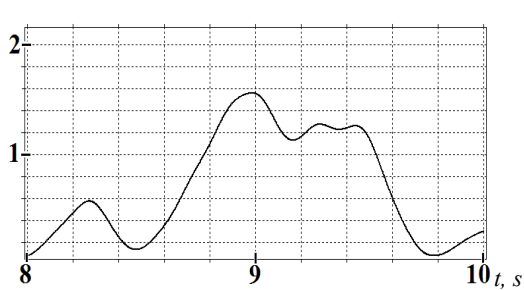


Figure 6e: Spectral integral in the channel  $P_z$  (8.982;1.56) in the interval [8–9.15 s].

$E_{\alpha}(J; t)$

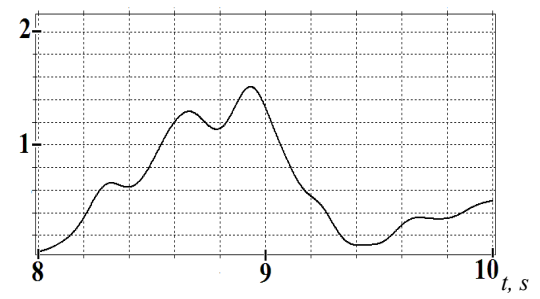


Figure 6i: Spectral integral in the channel  $0_2$  (8.934;1.514) in the interval [8–9.15 s].

Fig.6 shows the behavior of spectral integrals  $E_\alpha(J; t)$  in all central channels  $J = \{C_3, C_z, C_4; P_3, P_z, P_4; O_1, O_z, O_2\}$  on a single scale in the interval [8–9.15 s]. The development of the burst during time interval [8–9.15 s] starts in the occipital channel  $O_1$ . Then it reaches a maximum in  $O_z$ , and, gradually decreasing in size, reaches the central channels  $P_4$  and  $P_z$ . After that, the burst arrives into the channel  $C_4$ , decreasing in amplitude by 2.6 times compared with the maximum in  $O_z$ . In addition, the maximum of the burst from the channel  $P_z$  moves along the trajectory  $C_3 \rightarrow P_3 \rightarrow C_z$  (Fig.7). So, the disturbance spreads from occipital to central and parietal regions with its activity decreasing in time.

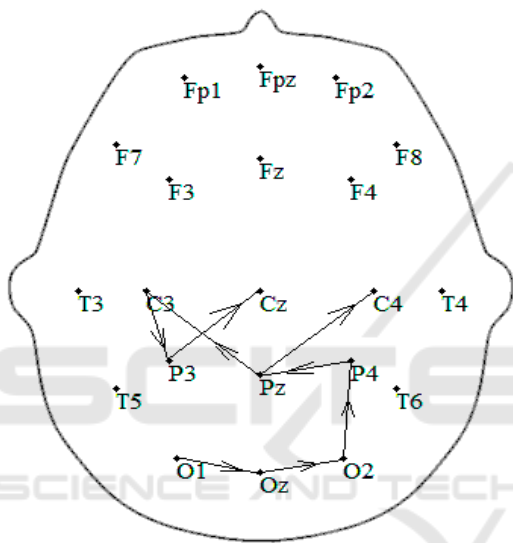


Figure 7: The trajectory of the burst activity maximum in the time interval [8-9.15 s].

This can be considered as a certain wave process associated with the excitation of local neural ensembles caused by some stimuli.

It is important to note that for the peripheral channels  $J = \{F_7; F_8; T_3; T_4; T_5; T_6\}$  the values of  $E_\alpha(J, t)$  in  $\alpha$ -range fall by more than  $e = 2,72$  times as compared to the maximum value of the burst observed in the central occipital. The numerical values  $E(J, t_{max})$  are given for each  $J$ , where  $t_{max}$  is the time moment in seconds at which the maximum value of the spectral integral for the given channel is reached. Figures 6 show that the intensities and shapes of bursts are different for each channel. Moreover, the maximums of the bursts also vary in amplitude and time localization, so we may talk about bursts moving at a certain speed along their own path, that is, about a wave propagating in a dispersive medium. The study of Fig.6 makes it possible to find

the trajectories of the maxima of the bursts along the cerebral cortex. This can be done, if we trace the maxima of the corresponding spectral integrals in different channels and connect them.

A different trajectory characterizes the burst in [16.3-17.2 s] (Fig.8-9). The burst of small amplitude (0.844) occurs in the central channel  $C_z$ . This burst also reaches its maximum value (2.664) in  $O_z$ . A careful analysis of the shape of the bursts in Fig.4, Fig.5 shows that an individual burst often has a complex shape and consists of several peaks. In this case, the trajectories of the burst maximum do not take into account the changes in the intensity maxima redistribution of inside the burst itself. It turns out that in the case of approximating the total burst  $E_\alpha(J, t)$  by the mathematical model (2), the velocities, amplitudes, and widths of each Gaussian peak appeared to be individual.

The results of calculation of spectral integrals  $E_\alpha(J; t)$  for different EEG channels in the time interval [16.3-17.2 s] are shown in Fig.8.

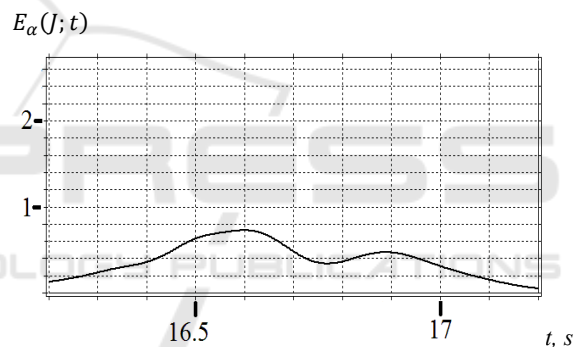


Figure 8a: Spectral integral in the channel  $C_3$  (16.600;0,726) in the interval [16.3-17.2 s].

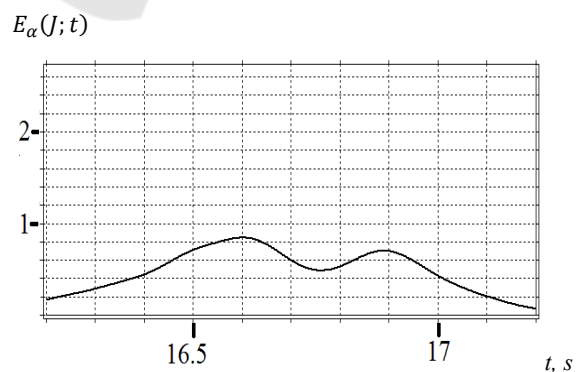


Figure 8b: Spectral integral in the channel  $C_z$  (16.602;0,844) in the interval [16.3-17.2 s].

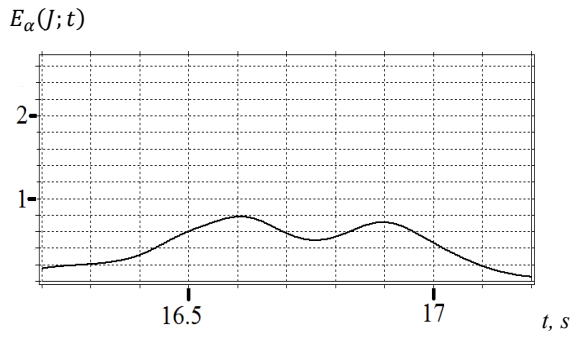


Figure 8c: Spectral integral in the channel C<sub>4</sub> (16.606;0,78) in the interval [16.3-17.2 s].

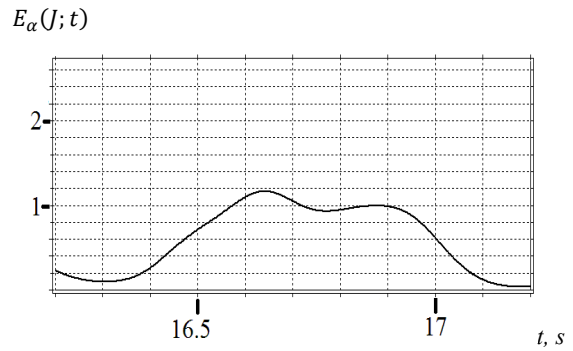


Figure 8g: Spectral integral in the channel O<sub>1</sub> (16.640;1,164) in the interval [16.3-17.2 s].

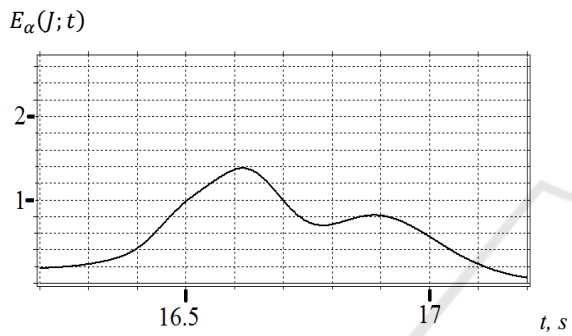


Figure 8d: Spectral integral in the channel P<sub>3</sub> (16.616;1,378) in the interval [16.3-17.2 s].

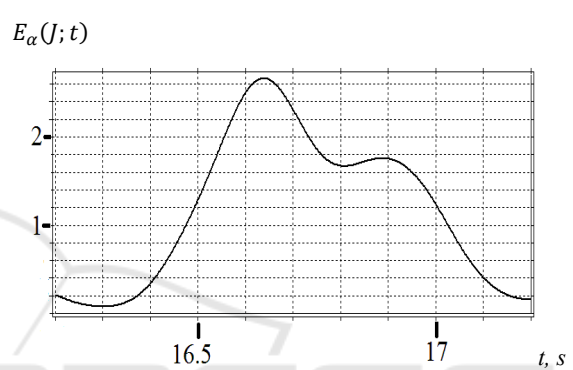


Figure 8h: Spectral integral in the channel O<sub>2</sub> (16.638;2,664) in the interval [16.3-17.2 s].

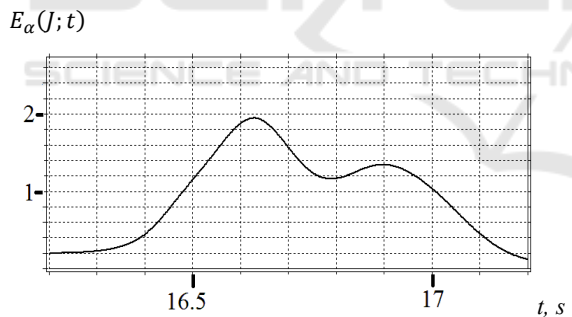


Figure 8e: Spectral integral in the channel P<sub>z</sub> (16.628;1,947) in the interval [16.3-17.2 s].

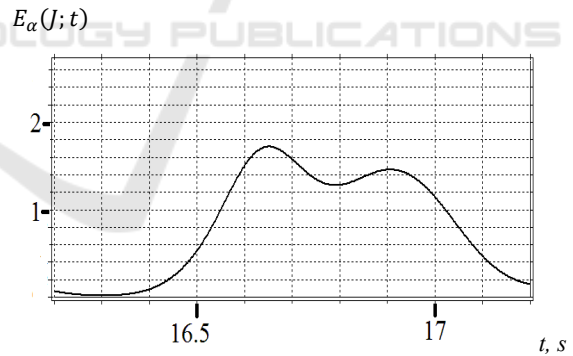


Figure 8i: Spectral integral in the channel O<sub>4</sub> (16.650;1,721) in the interval [16.3-17.2 s].

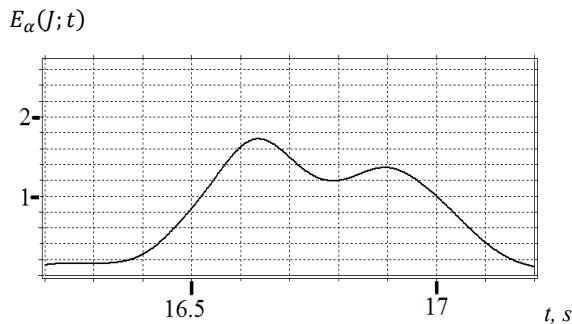


Figure 8f: Spectral integral in the channel P<sub>4</sub> (16.636;1,722) in the interval [16.3-17.2 s].

Just like the Figures 6, the Figures 8 show significant change in intensities and shapes of bursts in different EEG channels. The maximums of the bursts also vary in amplitude and time of occurrence, which indicates the movement of an excitement along the brain cortex.



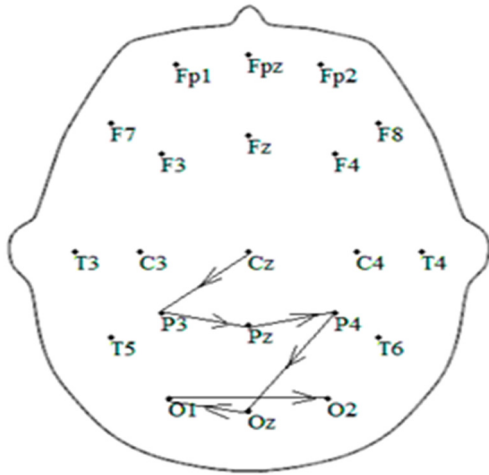


Figure 9: The trajectory of the burst activity maximum in the time interval [16.3-17.2 s].

## 2.4 Discussion and Conclusion

In this paper, we propose the mathematical model of EEG bursts propagating over the cerebral cortex as a combination of Gaussian peaks with their centers moving along different trajectories at different speeds. Each Gaussian peak in the burst is characterized by its amplitude, maximum in time and width. In accordance with the nonlinear approximation model, we approximate each burst by the sum of three Gaussian peaks with vectors  $\vec{g}_i = (a_i; b_i; c_i)$ , where  $i = 1, 2, 3$ . Calculating the parameters of each burst makes it possible to determine changes in the amplitude, shape, direction of motion, and velocity of the whole burst.

For mapping the movement of bursts over the cerebral cortex, we used continuous wavelet transform (CWT) with the Morlet mother wavelet function, and the temporary analysis of spectral integrals. By the method of CWT, the spectral integrals  $E_\mu(t)$  of non-stationary EEG signal have been calculated for each brain channel  $J$  in all frequency ranges  $\mu = \{\alpha, \beta, \gamma, \delta\}$ . The advantage of CWT applied in this work over the traditional window Fourier transform is that the latter requires the choice of window size  $W$ , which is the additional problem. For CWT the window size is adjusted automatically depending on the frequency  $\nu$ . When studying signals at low frequencies, the window becomes wide. In the high-frequency part of the spectrum ( $\alpha$  and  $\beta$  rhythms), the window becomes narrow. In the case when the EEG signal is a superposition of several non-stationary signals with a wide spread in characteristic durations and

frequencies, the choice of a single value  $W$  optimal for all spectral components  $\mu$  may not be possible at all.

The spectral integrals  $E_\mu(t)$  used in this work represent the value of the local density of the signal spectrum integrated over a certain frequency range  $\mu$ . An EEG record is presented as some non-stationary signal – a sequence of bursts, each of which is characterized by its spectral composition, beginning and end, and also by the time of electrical activity maximum. By using the EEG analysis in  $\alpha$ -range as an example, it is shown that there are various scenarios for the appearance and propagation of bursts in the cerebral cortex. Comparing the propagation of two bursts, we detected that in one  $\alpha$ -burst, an increase in perturbation occurs from the parietal region of the brain to the occipital. In another burst, the disturbances spread from the occipital region. Such a burst fades in the parietal and central brain channels. Based on the calculation of  $E_\alpha(t)$ , the map of activity in those areas of the brain, where the bursts reach the maximum values, is defined.

In the article (Anodina-Andrievskaya EM et al 2011) on the correlations of various EEG channels at solving cognitive problems, it was shown that the correlation map is individual for each person. We may assume that the map of velocities and directions of motion (Fig.7, 9) is individual for each person too. The intensity of the activity bursts and their localization in time and space recorded in EEG and ECoEG reflects the spatio-temporal picture of local neural ensembles reorganization.

The method of tracking the path of the disturbance propagation over the cerebral cortex can have many applications. It can be applied in the quantitative analysis and classification of transients that characterize the properties of the central nervous system of a person at the macro level. The method of restoring the movement of perturbation along the surface of the brain was used to determine the dynamics of assimilation and forgetting the rhythm of photo-stimulation for non-stationary EEG under the influence of flash. Thus, the mathematical techniques proposed in the article are the tool for processing numerous experimental data related to both the diagnosis of diseases and the study of cognitive processes in the human brain.

## ACKNOWLEDGEMENT

State Task for Basic Research (topic code FSEG-2020-0024).

## REFERENCES

- Alexander DM, Jurica P, Trengove C, Nikolaev AR, Gepshtein S, Zvyagintsev M, Mathiak K, Schulze-Bonhage A, Ruescher JA, Ball T, Leeuwen C (2013) Traveling waves and trial averaging: The nature of single-trial and averaged brain responses in large-scale cortical signals. *NeuroImage*, 73, 95–112
- Anodina-Andrievskaya EM, Bozhokin SV, Polonsky Yu Z, Suvorov NB, Marusina MY (2011) Perspective approaches to analysis of informativity of physiological signals and medical images of human intelligence. *Journal of Instrumental Engineering*, 54(7), 27-35
- Bahramisharif A, Gerven MAJ, Aarnoutse EJ, Mercier MR, Schwartz TH, Foxe JF, Ramsey NF, Jensen OJ (2016) Propagating Neocortical Gamma Bursts Are Coordinated by Traveling Alpha Waves. *Journal of Neuroscience*, 33(48), 18849-18854
- Belov DR, Kolodyazhnyi SF, Smit NYu (2004) Expression of Hemispheric Asymmetry and Psychological Type in the EEG Traveling Wave. *Human Physiology*, 30(1), 5-19
- Belov DR, Volnova AV, Ahmediev D (2016) Travelling wave of ECoG epileptic activity in local cortical seizure modeling in awake rats. *Journal of Higher Nervous Activity*, 66(6), 751-762
- Bozhokin SV (2010) Wavelet analysis of learning and forgetting of photostimulation rhythms for a nonstationary electroencephalogram. *Technical Phys*, 55(9), 1248-1256
- Bozhokin SV, Suvorov NB (2008) Wavelet analysis of transients of an electroencephalogram at photostimulation. *Biomed. Radioelectron*, N3, 21-25
- Bozhokin SV, Suslova IB (2014) Analysis of nonstationary HRV as a frequency modulated signal by double continuous wavelet transformation method. *Biomedical Signal Processing and Control*, 10, 34-40
- Bozhokin SV, Suslova IB (2015) Wavelet-based analysis of spectral rearrangements of EEG patterns and of nonstationary correlations. *Physica A: Statistical Mechanics and its Applications*, 421(1), 151–160
- Bozhokin SV, Zharko SV, Larionov NV, Litvinov AN, Sokolov IM (2017) Wavelet Correlation of Nonstationary Signals. *Technical Physics*, 62(6), 837-845. <https://doi.org/10.1134/S1063784217060068>
- Borisyuk R, Kazanovich Y (2006) Oscillations and waves in the models of interactive neural populations. *Biosystems*, 86, 53-62
- Buschman TJ, Denovellis EL, Diogo C, Bullock D, Miller EK (2012) Synchronous oscillatory neural ensembles for rules in the prefrontal cortex. *Neuron*, 76(1), 838-846
- Getmanenko OV, Belov DR, Kanunikov IE, Smit NY, Sibarov DA (2006) Reflection of cortical activation pattern in the human EEG phase structure. *Russian Journal of Physiology*, 92(8), 930-948
- Chizhov AV, Graham LJ (2008) Efficient evaluation of neuron populations receiving colored-noise current based on a refractory density method. *Phys.Rev. E*, 77, 011910
- Gnezditskii VV (2004) A Reverse EEG Problem and Clinical Electroencephalography. MEDpress-inform, Moscow
- Ivanitsky AM, Ivanitsky GA, Nikolaev AR, Sysoeva OV (2009) Encyclopedia of Neuroscience. Electroencephalography, Springer
- Hramov AE, Koronovskii AA, Makarov VA, Pavlov AN, Sitnikova E (2015) Wavelets in neuroscience. Springer Series in Synergetics, Springer-Verlag, Berlin, Heidelberg
- Kaplan A, Borisov SV (2003) Dynamic properties of segmental characteristics of EEG alpha activity in rest conditions and during cognitive tasks. *Zhurnal Vyssei Nervnoi Deiatelnosti*, 53(1), 22-32
- Kulaichev AP (2011) The informativeness of coherence analysis in EEG studies. *Neuroscience and behavioral physiology*, 41(3), 321-328
- Lopes da Silva F (1991) Neural mechanisms underlying brain waves: from neural membranes to networks. *Electroenceph. Clin. Neurophysiol*, 79, 81–93
- Manjarrez E, Vázquez M, Flores A (2007) Computing the center of mass for traveling alpha waves in the human brain. *Brain Research*, 1145, 239 – 247
- Massimini M, Huber R, Ferrarelli F, Hill S, Tononi G (2004) The Sleep Slow Oscillation as a Traveling Wave. *Neurosci.*, 24(31), 6862– 6870
- Muller L, Chavane F, Reynolds J, Sejnowski TJ (2018) Cortical travelling waves: mechanisms and computational principles. *Nature Reviews Neuroscience*, 19(5), 255–268. <https://doi.org/10.1038/nrn.2018.20>
- Mysin IE, Kitchigina VF, Kazanovich YJ (2015) Modeling synchronous theta activity in the medial septum: Key role of local communications between different cell populations. *Journal of Computational Neuroscience*, 39, 1-16. <https://doi.org/10.1007/s10827-015-0564-6>
- Ng V, Barker GJ, Hendler T (2003) Psychiatric Neuroimaging, Series 1: Life and Behavioural Science, V.348 of NATO Science Series
- Nikolaev AR, Ivanitskii GA, Ivanitskii AM (2001) Studies of Cortical Interactions over Short Periods of Time during the Search for Verbal Associations. *Physiology, Neuroscience and Behavioral Physiology*, 31(2), 119-132
- Nunez PL (2000) Towards a quantitative description of large-scale neocortical dynamic function and EEG. *Behavioral and brain sciences*, 23, 371–437
- Nunez PL, Srinivasan R (2006) Electric Fields of the Brain: The Neurophysics of EEG, second ed., Oxford University Press
- Ozaki TJ, Sato N, Kitajo K, Someya Y, Anami K, Mizuhara H, Ogawa S, Yamaguchi Y (2012) Traveling EEG slow oscillation along the dorsal attention network initiates spontaneous perceptual switching. *Cognitive Neurodynamics*, 6, 185–198
- Patten TM, Rennie CJ, Robinson PA, Gong P (2012) Human Cortical Traveling Waves: Dynamical Properties and Correlations with Responses. *PLoS ONE*, 7(6), e38392

- Pfurtscheller G, Lopes da Silva FH (1999) Event-related EEG/MEG synchronization and desynchronization: basic principles. *Clinical Neurophysiology*, 110, 1842-1857
- Quiles MG, Wang D, Zhaoc L, Romeroc RAF, Huang DS (2011) Selecting salient objects in real scenes: An oscillatory correlation model. *Neural Networks*, 24, 54-64
- Riedner BA, Vyazovskiy VV, Huber R, Massimini M, Esser S, Murphy M, Tononi G (2007) Sleep homeostasis and Cortical Synchronization. III. A high-density EEG Study of Sleep Slow Waves in Humans. *Sleep*, 30(12), 1643-1657
- Tafreshi TF, Daliri MR, Ghodousi M (2019) Functional and effective connectivity-based features of EEG signals for object recognition. *Cognitive Neurodynamics*, 13(6), 555-566
- Trofimov AG, Kolodkin IV, Ushakov LV, Velichkovskii BM (2015) Agglomerative method for isolating microstates EEG related to the characteristics of the traveling wave. *Neuroinformatic-2015, MIFI, Moscow, Part 1*. P. 66-77
- Terman DH, Ermentrout GB, Yew AC (2001) Propagating activity patterns in thalamic neuronal networks. *SIAM Journal on Applied Mathematics*, 61, 1578-1604
- Tong S, Thakor NN (2009) *Quantitative EEG Analysis Methods and Clinical Applications*. Artech House. Boston. London
- Verkhlyutov VM, Balaev VV, Ushakov VL, Velichkovsky BM (2019) A Novel Methodology for Simulation of EEG Traveling Waves on the Folding Surface of the Human Cerebral Cortex. *Studies in Computational Intelligence*, 799, 51-63. [https://doi.org/10.1007/978-3-030-01328-8\\_4](https://doi.org/10.1007/978-3-030-01328-8_4)
- Villacorta-Atienza JA, Makarov VA (2013) Wave-Processing of Long-Scale Information by Neuronal Chains. *PLoS ONE* 8(2), e57440. <https://doi.org/10.1371/journal.pone.0057440>
- Voytek B, Canolty R, Shestyuk A, Crone N, Parvizi J, Knight R (2010) Shifts in gamma phase-amplitude coupling frequency from theta to alpha over posterior cortex during visual tasks. *Frontiers in Human Neuroscience*, 4, 191
- Zenkov LR (2013) *Clinical Electroencephalography*, MEDpress-inform
- Zhang H, Watrous AJ, Patel A, Jacobs J (2018) Theta and alpha oscillations are traveling waves in the human neocortex. *Neuron*, 98(6), 1269-1281. <https://doi.org/10.1016/j.neuron.2018.05.019>